Discussing direct search of dark matter particles in the minimal supersymmetric extension of the standard model with light neutralinos

N. Fornengo, S. Scopel,[2] and A. Bottino[1]

[1]*Dipartimento di Fisica Teorica, Università di Torino Istituto Nazionale di Fisica Nucleare, Sezione di Torino via P. Giuria 1, I–10125 Torino, Italy*

[2]*Department of Physics, Sogang University Seoul, Korea, 121-742*

(Received 26 November 2010; published 6 January 2011)

We examine the status of light neutralinos in an effective minimal supersymmetric extension of the standard model at the electroweak scale which was considered in the past and discussed in terms of the available data of direct searches for dark matter particles. Our reanalysis is prompted by new measurements at the Tevatron and B factories which might potentially provide significant constraints on the minimal supersymmetric extension of the standard model. Here we examine in detail all these new data and show that the present published results from the Tevatron and B factories have only a mild effect on the original light-neutralino population. This population, which fits quite well the DAMA/LIBRA annual modulation data, would also agree with the preliminary results of CDMS, CoGeNT, and CRESST, should these data, which are at present only hints of excesses of events over the expected backgrounds, be interpreted as authentic signals of dark matter. For the neutralino mass we find a lower bound of 7–8 GeV. Our results differ from some recent conclusions by other authors because of a few crucial points which we try to single out and elucidate.

DOI: 10.1103/PhysRevD.83.015001 PACS numbers: 95.35.+d, 11.30.Pb, 12.60.Jv, 95.30.Cq

I. INTRODUCTION

Much interest has recently been raised by some new hints of possible signals of dark matter (DM) particles in experiments of direct detection (CDMS [1], CoGeNT [2], CRESST [3]) which previously reported upper bounds only. These hints are in fact only constituted by excesses of events over what would be expected from backgrounds. What is intriguing is that these events, if actually due to DM particles with a coherent interaction with the atomic nuclei of the detector material, would be concentrated in a physical region which, expressed in terms of the weakly interacting massive particle (WIMP) mass and of the WIMP-nucleon elastic cross section, agrees with the physical region established with a high statistical significance by the DAMA Collaboration from a measurement of annual modulation over 13 yearly cycles with the DAMA/NaI and the DAMA/LIBRA experiments [4].

These results have prompted a large number of phenomenological papers focussed on WIMPs with a light mass (around 10 GeV) and a WIMP-nucleon elastic cross section of order $(10^{-40}$–$10^{-41})$ cm^2, whereas previous theoretical and experimental considerations were prevalently directed toward physical regions with much higher masses and lower cross sections. Turning to a specific candidate, it has now become common to consider neutralinos of light mass ($\sim$ 10 GeV).

Actually, already long ago in Ref. [5] it was stressed that, in case of R-parity conservation, a light neutralino (i.e., a neutralino with $m_\chi \lesssim 50$ GeV), when it happens to be the lightest supersymmetric particle, constitutes an extremely interesting candidate for the dark matter in the Universe, with direct detection rates accessible to experiments of the present generation. In Ref. [5] a lower bound of $m_\chi \sim 7$ GeV was also derived from the cosmological upper limit on the cold dark matter density. The theoretical framework, considered in Ref. [5], which allows neutralinos with a mass in the range 7 GeV $\lesssim m_\chi \lesssim 50$ GeV is an effective minimal supersymmetric extension of the standard model (MSSM) at the electroweak (EW) scale, where the usual hypothesis of gaugino-mass unification at the scale of grand unification of the SUperGRAvity (SUGRA) models, is removed; this effective MSSM is very manageable, since expressible in terms of a limited number of independent parameters. This model is the theoretical basis we also adopt for the phenomenological investigations presented in this work (for simplicity, the model which entails low-mass ($m_\chi \lesssim 50$ GeV) neutralino configurations within this effective MSSM will hereby be dubbed the light-neutralino model [LNM]); its main features are briefly summarized in Sec. II.

When the DAMA Collaboration published their experimental results collected with a NaI detector of 100 kg over 7 annual cycles [6], in Ref. [7] it was proved that indeed the population of light neutralinos [5] fitted well with these data. The possible interpretation of the annual modulation results in terms of light neutralinos was further confirmed in Refs. [8,9], when the channeling effect was taken into account in the experimental analysis [10] and the first DAMA/LIBRA combined data were presented [11].

We recall that the present collection of data by the same collaboration [4] amounts to an exposure of 1.17 ton$\times$ year, with evidence for an annual modulation effect at 8.9σ C.L. This extended collection of data entails that

the DAMA/LIBRA annual modulation regions in the plane WIMP mass–WIMP-nucleon scattering cross section, reported in the figures of Ref. [9] with a comparison with the theoretical predictions within LNM, essentially maintain their shapes, but with a statistical significance increased from 6.5σ to 7.5σ (see Ref. [9] for a detailed definition of these regions).

As mentioned above, other experimental collaborations have recently reported some events that might be in excess of the expected backgrounds. Two candidate events for dark matter, which would survive after application of various discrimination and subtraction procedures, were reported by the CDMS Collaboration [1]. In Ref. [12] it is shown that, should these events be actually due to dark matter, they would be compatible with light neutralinos and the DAMA results. Likewise, compatible with the LNM and the previously quoted experimental data, would be the excess of bulklike events reported by the CoGeNT Collaboration [2], again in case these might actually be significant of a DM effect. Most recently, the CRESST Collaboration has also presented results which, if interpreted as due to DM particles, would point to WIMPs with a mass $\lesssim 15$ GeV and a scalar WIMP-nucleon cross section in the ballpark of the previous experiments [3].

As previously mentioned, the new experimental results of Refs. [1–3], combined with the DAMA data, have recently triggered a large number of phenomenological considerations on coherently interacting WIMPs of light mass (see for instance Refs. [13–24]), with emphasis for the mass range 7–10 GeV. We wish to stress that, though this is a very interesting mass interval, already pointed out in Refs. [5,7–9], the physical region compatible with the DAMA results alone and accessible, in particular, to relic neutralinos is much wider; its specific size depends on a number of astrophysical features (e.g., WIMP distribution function in the galactic halo) and on the detector response (role of the channeling effect in detectors which use crystals [25]). For instance, it was shown in Ref. [9] that for the case of a WIMP halo distribution given by a cored-isothermal sphere the extended mass range is $7\ \text{GeV} \lesssim m_\chi \lesssim 60$ GeV. In view of the high significance of the annual modulation results versus the still preliminary character of the hints of the experiments in Refs. [1–3], we will consider in the present paper the status of relic neutralinos in the whole WIMP light-mass range $7\ \text{GeV} \lesssim m_\chi \lesssim 50$ GeV, as we did in our previous publications on light neutralinos.

Our present investigation is mainly focussed on the role that recent measurements at the Tevatron and at the B factories *BABAR* and Belle can have in providing constraints on supersymmetric models more stringent than the ones previously considered in Ref. [9]. Specifically, we consider the new data concerning the following processes: (a) the decay $B_s \to \mu^- + \mu^+$, the top-to-bottom quark decay with emission of a charged Higgs ($t \to b + H^+$), and the searches for neutral Higgs bosons into a tau-lepton pair, at the Tevatron; (b) the rare decays $B \to \tau + \nu_\tau$ and $B \to D + \tau + \nu_\tau$ (and $B \to D + l + \nu_l$, where $l = e, \mu$), at the B factories *BABAR* and Belle.

These measurements have potentially a significant role in constraining the supersymmetric parameter space in the region of high $\tan\beta$ and of light Higgs masses and consequently in determining the allowed ranges for a number of crucial quantities: neutralino relic abundance, lower bound on the neutralino mass and elastic neutralino-nucleon cross section. Here the nature of these constraints is critically analyzed, taking also into account the fact that many of them are still affected by sizable uncertainties. Their impact in constraining the parameter space of our supersymmetric model is investigated in a twofold way: by analytic investigations and by detailed numerical analyses. We believe that the analytic derivations are necessary: (i) to clarify how the relevant physical quantities mentioned above depend on the parameters of the LNM, (ii) to establish the impact that each specific constraint has on these model parameters and then consequently on the physical quantities, (iii) to direct the numerical analyses to the regions of the parameter space which are of most relevance, (iv) to interpret the outcomes of the numerical evaluations correctly and, finally, (v) to serve as a guide for an educated guess about how the present situation could evolve, as new experimental limits on supersymmetric parameters from accelerator experiments and other precision measurements might become available in the future.

In the course of our discussion we will also comment on how our results compare with some of the outcomes of other recent papers where numerical analyses of the previously mentioned constraints have been discussed (see, for instance, Refs. [15,16,21–23,27]).

The scheme of our paper is the following. In Sec. II the main features of our effective supersymmetric model are presented. In Sec. III we derive from the analytic expression of the neutralino relic abundance the lower bound for the neutralino mass in a form which displays its dependence on the main model parameters. Then in Sec. V we derive an approximate expression for the neutralino-nucleon cross section, which provides an easy estimate for this quantity. In Sec. VI we give an overview of the most relevant constraints which can have an impact on the ranges of our model parameters. Our evaluations are compared to the current results from experiments of direct DM particles in Sec. VII. We draw our conclusions in Sec. IX.

II. LIGHT NEUTRALINOS IN AN EFFECTIVE MSSM (LNM)

The supersymmetric scheme we employ in the present paper is the one described in Ref. [5]: an effective MSSM scheme at the electroweak scale, with the following independent parameters: $M_1, M_2, M_3, \mu, \tan\beta, m_A, m_{\tilde{q}}, m_{\tilde{l}}$, and A. We stress that the parameters are defined at the EW scale. Notations are as follows: M_1, M_2 and M_3 are the

U(1), SU(2) and SU(3) gaugino masses (these parameters are taken here to be positive), μ is the Higgs mixing mass parameter, $\tan\beta$ the ratio of the two Higgs vacuum expectation values, m_A the mass of the CP-odd neutral Higgs boson, $m_{\tilde{q}}$ is a squark soft mass common to all squarks, $m_{\tilde{l}}$ is a slepton soft mass common to all sleptons, and A is a common dimensionless trilinear parameter for the third family, $A_{\tilde{b}} = A_{\tilde{t}} \equiv A m_{\tilde{q}}$ and $A_{\tilde{\tau}} \equiv A m_{\tilde{l}}$ (the trilinear parameters for the other families being set equal to zero). In our model, no gaugino-mass unification at a grand unified scale is assumed.

The following experimental constraints are imposed: accelerators data on supersymmetric and Higgs boson searches at the CERN e^+e^- collider LEP2 [28]; the upper bound on the invisible width for the decay of the Z-boson into non-standard model particles: $\Gamma(Z \to \chi\chi) < 3$ MeV [29,30] (the role of this bound will be discussed in Sec. III A); measurements of the $b \to s + \gamma$ decay process [31]: $2.89 \leq BR(b \to s\gamma) \cdot 10^4 \leq 4.21$ is employed here (this interval is larger by 25% with respect to the experimental determination [31] in order to take into account theoretical uncertainties in the supersymmetric (SUSY) contributions [32] to the branching ratio of the process (for the standard model (SM) calculation, we employ the next-to next-to-leading order results from Ref. [33]); the measurements of the muon anomalous magnetic moment $a_\mu \equiv (g_\mu - 2)/2$: for the deviation, $\Delta a_\mu \equiv a_\mu^{\rm exp} - a_\mu^{\rm the}$, of the experimental world average from the theoretical evaluation within the SM we use here the (2σ) range $31 \leq \Delta a_\mu \cdot 10^{11} \leq 479$, derived from the latest experimental [34] and theoretical [35] data (the supersymmetric contributions to the muon anomalous magnetic moment within the MSSM are evaluated here by using the formulae in Ref. [36]; the constraints on the SUSY parameters obtained from the searches for the neutral Higgs boson at the Tevatron [37–39]; the upper bound (at 95% C.L.) on the branching ratio for the decay $B_s \to \mu^+ + \mu^-$: $BR(B_s \to \mu^+\mu^-) < 5.8 \times 10^{-8}$ [40] and the constraints related to $\Delta M_{B,s} \equiv M_{B_s} - M_{\bar{B}_s}$ [41,42]. The role of these two last categories of bounds in constraining the LNM is elucidated in Sec. VI A, while the constraints from the searches for neutral Higgs bosons at the Tevatron are discusses in Sec. VI B. The cosmological upper bound on cold dark matter (CDM), which is also implemented in our calculations, is discussed in Sec. III. Other possible constraints from the Tevatron and B factories are analyzed in detail in Sec. VI.

The linear superposition of bino $\tilde{B}$, wino $\tilde{W}^{(3)}$ and of the two Higgsino states $\tilde{H}_1^\circ$, $\tilde{H}_2^\circ$ which defines the neutralino state of lowest mass m_χ is written here as

$$\chi \equiv a_1\tilde{B} + a_2\tilde{W}^{(3)} + a_3\tilde{H}_1^\circ + a_4\tilde{H}_2^\circ. \tag{1}$$

The properties of these states have been investigated in detail, analytically and numerically, in Ref. [43] for the case when the smallest mass eigenstate χ_1 (or χ in short) is light, i.e., $m_\chi \equiv m_{\chi_1} \lesssim 50$ GeV. Of that analysis we report here only the main points that are relevant for the present paper.

We first notice that the lowest value for m_χ occurs when

$$m_\chi \simeq M_1 \ll |\mu|, M_2, \tag{2}$$

since the LEP lower limit on the chargino mass ($m_{\chi^\pm} \gtrsim 100$ GeV) sets a lower bound on both $|\mu|$ and M_2: $|\mu|$, $M_2 \gtrsim 100$ GeV, whereas M_1 is unbound. Thus, χ is mainly a Bino; its mixings with the other interaction eigenstates are given by

$$\frac{a_2}{a_1} \simeq \frac{\xi_1}{M_2}\cot\theta_W, \tag{3}$$

$$\frac{a_3}{a_1} \simeq \sin\theta_W \sin\beta \frac{M_Z}{\mu}, \tag{4}$$

$$\frac{a_3}{a_4} \simeq -\frac{\mu \sin\beta}{M_1 \sin\beta + \mu\cos\beta}, \tag{5}$$

where $\xi_1 \equiv m_\chi - M_1$ and θ_W is the Weinberg angle. These expressions readily follow from the general analytical formulae given in Ref. [43] by taking $\tan\beta \geq 10$, as consistent with the scenarios discussed below.

From the above expressions, the following relevant property holds: χ is mainly a Bino whose mixing with $\tilde{H}_1^\circ$ is non-negligible at small μ. In fact, for the ratio $|a_3|/|a_1|$ one has

$$\frac{|a_3|}{|a_1|} \simeq \sin\theta_W \sin\beta \frac{M_Z}{|\mu|} \lesssim 0.43 \sin\beta, \tag{6}$$

where in the last step we have taken into account the experimental lower bound $|\mu| \gtrsim 100$ GeV.

It is also useful to explicit the connection between the neutralino mass m_χ and the parameter M_1 at small m_χ. From the diagonalization of the neutralino mass matrix, one finds

$$m_\chi = M_1 - \sin\theta_W M_Z\left(\frac{a_3}{a_1}\cos\beta - \frac{a_4}{a_1}\sin\beta\right). \tag{7}$$

Employing Eqs. (3)–(5), we obtain

$$\begin{aligned} m_\chi &\simeq M_1 - \sin^2\theta_W \frac{m_Z^2}{\mu^2}\left(\frac{2\mu}{\tan\beta} + M_1\right) \\ &\simeq M_1(1 - 0.16\mu_{100}^{-2}) - 1.1\mu_{100}\left(\frac{35}{\tan\beta}\right) \text{GeV}, \end{aligned} \tag{8}$$

or

$$M_1 \simeq \frac{1}{(1 - 0.16\mu_{100}^{-2})}\left[m_\chi + 1.1\left(\frac{35}{\tan\beta}\right)\mu_{100}\ \text{GeV}\right], \tag{9}$$

where μ_{100} denotes μ in units of 100 GeV.

III. COSMOLOGICAL BOUND AND LOWER LIMIT TO THE NEUTRALINO MASS

The neutralino relic abundance is given by

$$\Omega_\chi h^2 = \frac{x_f}{g_\star(x_f)^{1/2}} \frac{9.9 \cdot 10^{-28} \mathrm{cm}^3 \mathrm{s}^{-1}}{\langle \widetilde{\sigma_{\mathrm{ann}} v} \rangle}, \tag{10}$$

where $\langle \widetilde{\sigma_{\mathrm{ann}} v} \rangle \equiv x_f \langle \sigma_{\mathrm{ann}} v \rangle_{\mathrm{int}}$, $\langle \sigma_{\mathrm{ann}} v \rangle_{\mathrm{int}}$ being the integral from the present temperature up to the freeze-out temperature T_f of the thermally averaged product of the annihilation cross section times the relative velocity of a pair of neutralinos, x_f is defined as $x_f \equiv m_\chi / T_f$ and $g_\star(x_f)$ denotes the relativistic degrees of freedom of the thermodynamic bath at x_f. For $\langle \widetilde{\sigma_{\mathrm{ann}} v} \rangle$ we will use the standard expansion in S and P waves: $\langle \widetilde{\sigma_{\mathrm{ann}} v} \rangle \simeq \tilde{a} + \tilde{b}/(2x_f)$. Notice that in the LNM no coannihilation effects are present in the calculation of the relic abundance, due to the large mass splitting between the mass of the neutralino ($m_\chi < 50$ GeV) and those of sfermions and charginos.

In our numerical evaluations all relevant contributions to the pair annihilation cross section in the denominator of Eq. (10) are included. However, approximate expressions for $\Omega_\chi h^2$ can be derived analytically; these will prove to be very useful to obtain analytic formulae for the lower bound for the neutralino mass.

A. Scenario $\mathcal{A}$

We first analyze the case of small values for the mass of the CP-odd neutral Higgs boson m_A: 90 GeV $\leq m_A \leq$ 150 GeV. In this case the main contribution to $\langle \sigma_{\mathrm{ann}} v \rangle_{\mathrm{int}}$ is provided by the A exchange in the s channel of the annihilation process $\chi + \chi \rightarrow \bar{b} + b$ (one easily verifies that when $m_\chi < m_b$, $\langle \sigma_{\mathrm{ann}} v \rangle_{\mathrm{int}}$ entails a relic abundance exceeding the cosmological bound). Thus, one obtains [5]

$$\Omega_\chi h^2 \simeq \frac{4.8 \cdot 10^{-6}}{\mathrm{GeV}^2} \frac{x_f}{g_\star(x_f)^{1/2}} \times \frac{1}{a_1^2 a_3^2 \tan^2\beta} m_A^4 \frac{[1 - (2m_\chi)^2/m_A^2]^2}{m_\chi^2 [1 - m_b^2/m_\chi^2]^{1/2}} \frac{1}{(1+\epsilon_b)^2}, \tag{11}$$

where ϵ_b is a quantity that enters into the relationship between the b-quark running mass and the corresponding Yukawa coupling (see Ref. [44] and references quoted therein). In deriving this expression, one has taken into account that here the following hierarchy holds for the coefficients a_i of χ:

$$|a_1| > |a_3| \gg |a_2|, |a_4|, \tag{12}$$

as easily derivable from Eqs. (3)–(5).

As far as the value of $g_\star(x_f)^{1/2}$ is concerned, we notice that for light neutralinos $x_f \simeq 21$–22, so that neutralinos with masses $m_\chi \simeq 6$–7 GeV have a freeze-out temperature $T_f \sim T_{\mathrm{QCD}}$, where T_{QCD} is the hadron-quark transition temperature of order 100–300 MeV. For definiteness, we describe here the hadron-quark transition by a step function: if T_{QCD} is set equal to 300 MeV, then for $m_\chi \lesssim 6$ GeV one has $g_\star(x_f)^{1/2} \simeq 4$, while for heavier neutralinos $g_\star(x_f)^{1/2} \simeq 8$–$9$. In the approximate analytic expressions discussed hereafter, we set $x_f / g_\star(x_f)^{1/2} = 21/8$ (while in the numerical analysis the actual values obtained after solving the Boltzmann equation are used).

In selecting the physical parameter space for relic neutralinos, a first fundamental constraint to be applied is that the neutralino relic abundance does not exceed the observed upper bound for CDM, i.e., $\Omega_\chi h^2 \leq (\Omega_{\mathrm{CDM}} h^2)_{\mathrm{max}}$. If we apply this requirement, by using Eq. (11), we obtain the following lower bound on the neutralino mass:

$$m_\chi \frac{[1 - m_b^2/m_\chi^2]^{1/4}}{[1 - (2m_\chi)^2/m_A^2]} \gtrsim 7.4 \text{ GeV} \left(\frac{m_A}{90 \text{ GeV}}\right)^2 \left(\frac{35}{\tan\beta}\right) \times \left(\frac{0.12}{a_1^2 a_3^2}\right)^{1/2} \left(\frac{0.12}{(\Omega_{\mathrm{CDM}} h^2)_{\mathrm{max}}}\right)^{1/2}. \tag{13}$$

Here we have taken as default value for $(\Omega_{\mathrm{CDM}} h^2)_{\mathrm{max}}$ the numerical value which represents the 2σ upper bound to $(\Omega_{\mathrm{CDM}} h^2)_{\mathrm{max}}$ derived from the results of Ref. [45]. For ϵ_b, we have used a value which is representative of the typical range obtained numerically in our model: $\epsilon_b = -0.08$.

Equation (13), already derived in Ref. [5], is written here in a form that shows more explicitly how the lower limit on m_χ depends on the various model parameters. Notice, in particular, that this lower bound scales (roughly) as m_A^2 and $(\tan\beta)^{-1}$. It is obvious that the precise value for the lower limit has however to be ascertained by numerical evaluations which take into account all the intricate interferences of the various physical constraints over the model parameters.

The right-hand side of Eq. (13) can be expressed completely in terms of the independent parameters of our SUSY model. In fact, by using Eq. (4) at large $\tan\beta$ ($\sin\beta \simeq 1$) and taking into account that, because of Eq. (12), $a_1^2 \simeq 1 - a_3^2$, we can rewrite $a_1^2 a_3^2$ as

$$a_1^2 a_3^2 \simeq \frac{\sin^2\theta_W m_Z^2 \mu^2}{(\mu^2 + \sin^2\theta_W m_Z^2)^2} \simeq \frac{0.19 \mu_{100}^2}{(\mu_{100}^2 + 0.19)^2}. \tag{14}$$

From this formula and the LEP lower bound $|\mu| \gtrsim 100$ GeV, we obtain $(a_1^2 a_3^2)_{\mathrm{max}} \lesssim 0.13$.

An upper limit on a_3^2 and then on the product $a_1^2 a_3^2$ is also placed by the upper bound on the width for the Z-boson decay into a light-neutralino pair. This decay width is given by [46,47]

$$\Gamma(Z \rightarrow \chi\chi) = \frac{1}{12\pi} \frac{G_F}{\sqrt{2}} M_Z^3 [1 - (2m_\chi)^2/M_Z^2]^{3/2} (a_3^2 - a_4^2)^2. \tag{15}$$

Taking into account that $a_3^2 \gg a_4^2$,

$$\Gamma(Z \to \chi\chi) = 166 \text{ MeV}[1 - (2m_\chi)^2/M_Z^2]^{3/2} a_3^4. \quad (16)$$

Denoting by $\Gamma(Z \to \chi\chi)_{\rm ub}$ the upper bound to the invisible fraction of the Z-decay width, we finally obtain

$$a_3^2 \lesssim \left(\frac{\Gamma(Z \to \chi\chi)_{\rm ub}}{154 \text{ MeV}}\right)^{1/2}, \quad (17)$$

where we have used for the neutralino mass the value $m_\chi \simeq 10$ GeV.

If we take conservatively $\Gamma(Z \to \chi\chi) < 3$ MeV [29,30], from Eq. (17) we find $a_1^2 a_3^2 \lesssim 0.12$, a value which is extremely close to the upper bound $(a_1^2 a_3^2)_{\rm max} = 0.13$ derived above from Eq. (14) and the experimental lower limit on $|\mu|$. The value $a_1^2 a_3^2 = 0.12$ is the reference value for $a_1^2 a_3^2$ employed in Eq. (13). Notice that the upper bound on a_3^2, placed by the invisible width for $Z \to \chi + \chi$, scales with the square root of the upper limit on this quantity [see Eq. (17)]; furthermore, the lower bound on m_χ scales as $(a_1^2 a_3^2)^{-1/2}$ [see Eq. (13)]. Thus, the lower limit on the neutralino mass is only very mildly dependent on the actual value of the upper bound on $\Gamma(Z \to \chi\chi)$. For instance, taking $\Gamma(Z \to \chi\chi) < 2$ MeV instead of $\Gamma(Z \to \chi\chi) < 3$ MeV, would increase the lower bound on m_χ by a mere 10% [48].

The properties of the very light neutralinos of cosmological interest considered in this section delineate a specific scenario hereby denoted as *scenario* $\mathcal{A}$ [43]. Its main features are strongly determined by the requirement that the neutralino relic abundance satisfies the cosmological bound $\Omega_\chi h^2 \leq (\Omega_{\rm CDM} h^2)_{\rm max}$. From the approximate formula in Eq. (11) one finds that (i) m_A must be light, 90 GeV $\leq m_A \lesssim$ (200–300) GeV (90 GeV being the lower bound from LEP searches); (ii) $\tan\beta$ has to be large: $\tan\beta = 20$–45, (iii) the $\tilde{B} - \tilde{H}_1^\circ$ mixing needs to be sizeable, which in turn implies small values of μ: $|\mu| \sim$ (100–200) GeV [see Eq. (14)]. As will be discussed in Sec. VI A, the trilinear coupling is constrained, for neutralinos lighter than 10 GeV, to be in the interval $|A| \lesssim 0.6$, because of the upper bound to $BR(B_s \to \mu^+ + \mu^-)$. Equation (13) shows that in scenario $\mathcal{A}$, we expect a lower bound on the neutralino mass of the order of 7.5 GeV, if the parameter space which defines this scenario is allowed by the bounds on Higgs searches and B physics. We will show in the next sections that this result actually holds.

B. Scenario $\mathcal{B}$

When $m_A \gtrsim$ (200–300) GeV, the cosmological lower bound on $\langle\sigma_{\rm ann} v\rangle_{\rm int}$ can be satisfied by a pair annihilation process which proceeds through an efficient stau-exchange contribution (in the t, u channels). This requires that (i) the stau mass $m_{\tilde{\tau}}$ is sufficiently light, $m_{\tilde{\tau}} \sim 90$ GeV (notice that the current experimental limit is $m_{\tilde{\tau}} \sim 87$ GeV) and (ii) χ is a very pure Bino (i.e., $(1 - a_1^2) \sim \mathcal{O}(10^{-2})$).

The requirement (i) sets a constraint on the quantity $|\mu|\tan\beta$, because the experimental lower bounds on the sneutrino mass and on the charged slepton masses of the first two families imply a lower bound on the soft slepton mass: $m_{\tilde{l}} \gtrsim 115$ GeV. Thus, in order to make the request $m_{\tilde{\tau}} \sim 90$ GeV compatible with $m_{\tilde{l}} \gtrsim 115$ GeV, it is necessary that the off-diagonal terms of the sleptonic mass matrix in the eigenstate basis, which are proportional to $\mu\tan\beta$, are large. Numerically, one finds $|\mu|\tan\beta \sim 5000$ GeV. On the other side, the condition (ii) requires that $|a_3/a_1| \lesssim 10^{-1}$, i.e., according to Eq. (4), $|a_3/a_1| \simeq \sin\theta_W \sin\beta (M_Z/\mu) \lesssim 10^{-1}$. Combining this last expression with the condition $|\mu|\tan\beta \sim 5000$ GeV, one finds that $|\mu|$ and $\tan\beta$ are bounded by $|\mu| \gtrsim 500$ GeV, $\tan\beta \lesssim 10$. These bounds are somewhat weaker for values of the neutralino mass larger than ~15–18 GeV.

The previous arguments lead us to introduce *scenario* $\mathcal{B}$ [43], identified by the following sector of the supersymmetric parameter space: $M_1 \sim 25$ GeV, $|\mu| \gtrsim 500$ GeV, $\tan\beta \lesssim 10$; $m_{\tilde{l}} \gtrsim$ (100–200) GeV, $-2.5 \lesssim A \lesssim +2.5$; the other supersymmetric parameters are not *a priori* fixed. Within this scenario it follows from Eqs. (3)–(5) that the following hierarchy holds for the coefficients a_i:

$$|a_1| \gg |a_2|, |a_3|, |a_4|. \quad (18)$$

As derived in Ref. [5] the cosmological bound $\Omega_\chi h^2 \leq (\Omega_{\rm CDM} h^2)_{\rm max}$ provides the lower bound $m_\chi \gtrsim 22$ GeV, whose scaling law in terms of the stau mass and $(\Omega_{\rm CDM} h^2)_{\rm max}$ is approximately given by

$$m_\chi[1 - m_\tau^2/m_\chi^2]^{1/4} \gtrsim 22 \text{ GeV}\left(\frac{m_{\tilde{\tau}}}{90 \text{ GeV}}\right)^2 \times \left(\frac{0.12}{(\Omega_{\rm CDM} h^2)_{\rm max}}\right). \quad (19)$$

In general, one has conservatively to retain as a lower bound to m_χ the smaller of the two lower limits given separately in Eq. (13) and in Eq. (19). From these equations one finds that the lower bound of Eq. (13) is less stringent than the one of Eq. (19) as long as $m_A \lesssim 2m_{\tilde{\tau}}$. Because of the present experimental bounds on m_A, $\tan\beta$ and $m_{\tilde{\tau}}$ the lower absolute bound is the one derived from Eq. (13). We parenthetically note that the lower limits $m_\chi \gtrsim$ (15–18) GeV found in Refs. [49,50] are due to the assumption that m_A is very large ($m_A \sim 1$ TeV).

IV. NUMERICAL ANALYSIS OF THE LNM PARAMETER SPACE

In the present paper we are interested in discussing neutralinos with very light masses. We will therefore concentrate on scenario $\mathcal{A}$ only, and in our numerical analyses we perform a scanning of the supersymmetric parameter space dedicated to this scenario. We will denote this sector of the LNM parameter space as LNM $\mathcal{A}$.

The ranges of the MSSM parameters, appropriately narrowed in order to explore this scenario are $10 \leq \tan\beta \leq 50$, $100\ \text{GeV} \leq \mu \leq 150\ \text{GeV}$, $5\ \text{GeV} \leq M_1 \leq 50\ \text{GeV}$, $100\ \text{GeV} \leq M_2 \leq 1000\ \text{GeV}$, $250\,\text{GeV} \leq m_{\tilde{q}} \leq 1000\,\text{GeV}$, $100\ \text{GeV} \leq m_{\tilde{l}} \leq 3000\ \text{GeV}$, $90\ \text{GeV} \leq m_A \leq 120\ \text{GeV}$, $0 \leq A \leq 1$.

In our scenario the trilinear coupling A and the μ parameter are both always positive. This is actually due to the interplay between the constraints on $BR(b \to s\gamma)$ (which requires $\mu A > 0$) and on a_μ (which requires $\mu > 0$). In all the plots shown in the paper, all the experimental bounds discussed in Sec. II are applied: i.e., invisible Z width, Higgs searches at LEP and Tevatron, $BR(b \to s\gamma)$, muon anomalous magnetic moment a_μ, $BR(B_s \to \mu^+\mu^-)$, $\Delta M_{B,s}$, $BR(t \to bH^+)$, and the upper bound on the cosmological abundance $\Omega_\chi h^2$. Whenever we refer to "LNM-$\mathcal{A}$ scan," we intend the scan of the parameters space defined above, implemented by the experimental bounds quoted here.

As for the scan of the parameter space, we randomly sample the above intervals using a logarithmic scale. It is worth noticing here that, due to the nontrivial interplay of the different constraints on physical masses and couplings, the typical success rate of our sampling for obtaining neutralinos with mass less than 10 GeV is of order 10^{-5}–10^{-6}. In particular, in order to populate the scatter plots with a sizable number of points and in a uniform way, we have subdivided the above ranges in smaller intervals for the neutralino mass $m_\chi \simeq M_1$ and run our code until a similar number of allowed points were found in each subrange. Less focused scans of the parameter space may fail to find the allowed configurations, especially in the lower range of m_χ, as seems to be the case with some analyses in the literature [21].

All the numerical results shown in the paper refer to this special LNM-$\mathcal{A}$ scan. The only exception will be Fig. 25, where a more general scan of the effective MSSM will be presented. In that (unique) case, the parameters will be varied in the following intervals: $1 \leq \tan\beta \leq 50$, $100\ \text{GeV} \leq |\mu| \leq 1000\ \text{GeV}$, $5\ \text{GeV} \leq M_1 \leq \min(100, 0.5M_2)\ \text{GeV}$, $100\,\text{GeV} \leq M_2 \leq 1000\,\text{GeV}$, $80\ \text{GeV} \leq m_{\tilde{q}} \leq 3000\ \text{GeV}$, $80\ \text{GeV} \leq m_{\tilde{l}} \leq 3000\ \text{GeV}$, $90\ \text{GeV} \leq m_A \leq 1000\ \text{GeV}$, $-1 \leq A \leq 1$. The scan of Fig. 25 will therefore include both scenario $\mathcal{A}$ and scenario $\mathcal{B}$, as well as more general scenarios, with heavier neutralinos. Within the scan at higher neutralino masses described above we have imposed the condition $m_{\text{NLSP}} > 1.05 m_\chi$ (with NLSP = sfermions, charginos) in order to remove configurations where the relic abundance is determined by coannihilations between the neutralino and the next-to-lightest SUSY particle . Notice that in an effective MSSM coannihilations are due to accidental degeneracies between uncorrelated parameters. This is at variance with the SUGRA scenario, where strong correlations among the mass of the neutralino and of other SUSY particles are expected, in particular, regions of the parameter space.

Now it is convenient to have a first look at a scatter plot for the neutralino population within the LNM $\mathcal{A}$. This is provided by Fig. 1 where the scatter plot is represented in the plane $m_\chi - \tan\beta$. In evaluating this scatter plot all constraints specifically mentioned in Sec. II (including the upper bound on $BR(B_s \to \mu^+\mu^-)$ and the cosmological upper bound $\Omega_\chi h^2 \leq (\Omega_{\text{CDM}} h^2)_{\text{max}} = 0.12$) have been applied. Notice that $\Omega_\chi h^2$ has been evaluated using its full expression, and not simply with its approximate version given in Eq. (11). This figure shows how accurate is the bound given in Eq. (13), which is represented by the (red) solid line. From this figure it turns out that the lower bound on the neutralino mass is $m_\chi \gtrsim 7.5$ GeV, this value being obtained when $\tan\beta \simeq 40$ and $m_A \simeq 90$ GeV. We stress that the updated constraint on $BR(B_s \to \mu^+\mu^-)$ induces only a very slight modification in the neutralino mass lower bound of 6–7 GeV determined in Ref. [5]. This constraint will be further discussed in Sec. VI A.

In Fig. 2 we give a scatter plot for $\Gamma(Z \to \chi\chi)$ versus m_χ. From this plot one sees that actually the lower bound on the neutralino mass changes very little when the upper bound on the invisible fraction of the Z-boson width, shown by the horizontal solid line, is decreased from 3 MeV to about 2 MeV, as previously argued. Somewhat below this value the impact of the invisible Z width on the lower bound of variation of m_χ may be substantial.

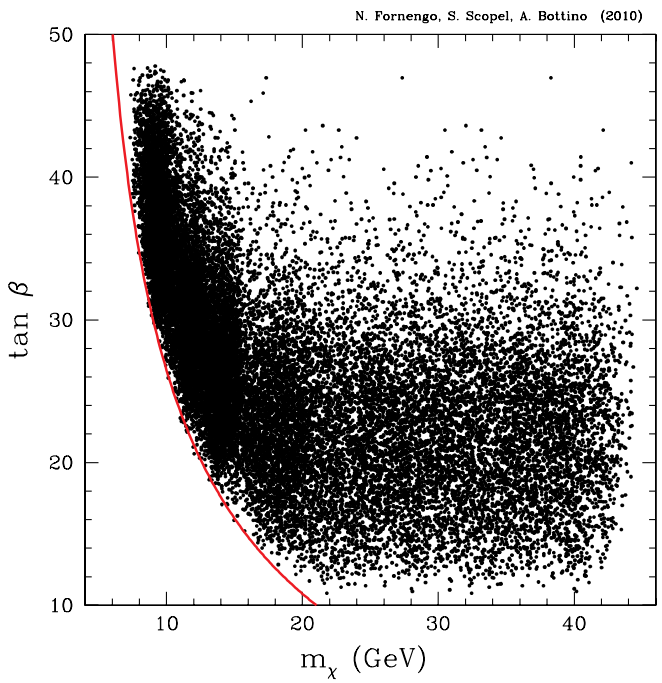

FIG. 1 (color online). Scatter plot of the light-neutralino population for the LNM-$\mathcal{A}$ scan, shown in the plane $m_\chi - \tan\beta$. The (red) solid line represents the analytic bound from the neutralino relic abundance given in Eq. (13).

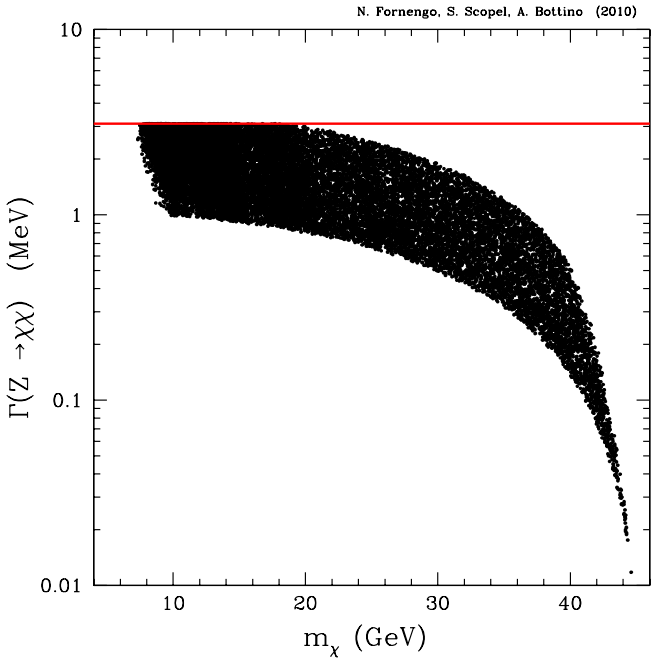

FIG. 2 (color online). Scatter plot for $\Gamma(Z \to \chi\chi)$ versus m_χ for the LNM-$\mathcal{A}$ scan. The (red) horizontal solid line denotes the present experimental upper bound to the invisible width of the Z decay into non-standard model particles.

V. NEUTRALINO-NUCLEON CROSS SECTION

In the present paper we analyze the results of present experiments searching for direct detection of DM particles, under the hypothesis that WIMPs have a dominant coherent interaction with the detector nuclei. This is the case for neutralinos. Once a specific distribution is assumed for the WIMPs in the halo, the WIMP-nucleus cross section can be immediately rewritten in terms of the WIMP-nucleon cross section; this is then the central quantity to be analyzed.

Thus, we turn now to an approximate evaluation of the neutralino-nucleon cross section in the case where the interaction process is due to exchange of the lighter CP-even neutral Higgs boson h. From the formulae in Refs. [51,52], one obtains

$$\sigma_{\text{scalar}}^{(\text{nucleon})} \simeq \frac{8G_F^2}{\pi} M_Z^2 m_{\text{red}}^2 \frac{F_h^2 I_h^2}{m_h^4}, \tag{20}$$

where

$$F_h = (-a_1 \sin\theta_W + a_2 \cos\theta_W)(a_3 \sin\alpha + a_4 \cos\alpha)$$
$$I_h = \sum_q k_q^h m_q \langle N|\bar{q}q|N\rangle. \tag{21}$$

The matrix elements $\langle N|\bar{q}q|N\rangle$ are meant to be over the nucleonic state, the angle α rotates $H_1^{(0)}$ and $H_2^{(0)}$ into h and H, and the coefficients k_q^h are given by

$$k_{u\text{-type}}^h = \cos\alpha/\sin\beta,$$
$$k_{d\text{-type}}^h = -\sin\alpha/\cos\beta - \epsilon_d \cos(\alpha-\beta)\tan\beta, \tag{22}$$

for the up-type and down-type quarks, respectively; ϵ_d has already been introduced in Eq. (11) for the case of the b quark.

Keeping the dominant terms (couplings of the Higgs boson h with the d-type quarks, $\alpha \simeq \pi/2$), one has

$$I_h \simeq k_{d\text{-type}}^h [m_d \langle N|\bar{d}d|N\rangle + m_s \langle N|\bar{s}s|N\rangle + m_b \langle N|\bar{b}b|N\rangle]$$
$$\simeq -\tan\beta g_d, \tag{23}$$

where

$$g_d \equiv [m_d \langle N|\bar{d}d|N\rangle + m_s \langle N|\bar{s}s|N\rangle + m_b \langle N|\bar{b}b|N\rangle]. \tag{24}$$

Thus,

$$\sigma_{\text{scalar}}^{(\text{nucleon})} \simeq 6.8 \times 10^{-7} a_1^2 a_3^2 \tan^2\beta \frac{g_d^2}{m_h^4}, \tag{25}$$

or

$$\sigma_{\text{scalar}}^{(\text{nucleon})} \simeq 5.3 \times 10^{-41}\ \text{cm}^2 \left(\frac{a_1^2 a_3^2}{0.13}\right)\left(\frac{\tan\beta}{35}\right)^2 \times \left(\frac{90\ \text{GeV}}{m_h}\right)^4 \left(\frac{g_d}{290\ \text{MeV}}\right)^2. \tag{26}$$

In this expression we have used as a *reference* value for g_d the value $g_{d,\text{ref}} = 290$ MeV employed in our previous papers [8,9]. We recall that this quantity is affected by large uncertainties [51] with $(g_{d,\max}/g_{d,\text{ref}})^2 = 3.0$ and $(g_{d,\min}/g_{d,\text{ref}})^2 = 0.12$ [9]. Our reference value $g_{d,\text{ref}} = 290$ MeV is larger by a factor 1.5 than the central value of Ref. [53], frequently used in the literature (see for instance Ref. [16]).

By employing Eq. (11) and Eq. (25), we obtain

$$(\Omega_\chi h^2)\sigma_{\text{scalar}}^{(\text{nucleon})} \simeq 3.3 \times 10^{-39}\ \text{cm}^2 g_d^2 \frac{[1-(2m_\chi)^2/m_A^2]^2}{m_\chi^2[1-m_b^2/m_\chi^2]^{1/2}} \times \frac{1}{(1+\epsilon_b)^2}. \tag{27}$$

From this expression we find that any neutralino configuration, *whose relic abundance stays in the cosmological range for CDM* (i.e., $(\Omega_{\text{CDM}}h^2)_{\min} \le \Omega_\chi h^2 \le (\Omega_{\text{CDM}}h^2)_{\max}$ with $(\Omega_{\text{CDM}}h^2)_{\min} = 0.098$ and $(\Omega_{\text{CDM}}h^2)_{\max} = 0.12$) and passes all particle-physics constraints, has an elastic neutralino-nucleon cross section of order

$$\sigma_{\text{scalar}}^{(\text{nucleon})} \simeq (2.7\text{–}3.4) \times 10^{-41}\ \text{cm}^2 \left(\frac{g_d}{290\ \text{MeV}}\right)^2 \times \frac{[1-(2m_\chi)^2/m_A^2]^2}{(m_\chi/(10\ \text{GeV})^2[1-m_b^2/m_\chi^2]^{1/2}}. \tag{28}$$

A few comments are in order here:

(i) The elastic cross section $\sigma_{\text{scalar}}^{(\text{nucleon})}$ is affected by large uncertainties because of the uncertainties inherent in the effective Higgs-quark coupling constant g_d [51].

Actually, $\sigma_{\rm scalar}^{\rm (nucleon)}$ is subject to an increase by a factor of 3.0 or to a decrease by a factor of 8.6 [9], as commented above;

(ii) Equation (28) shows that $\sigma_{\rm scalar}^{\rm (nucleon)}$ scales roughly as $(m_\chi)^{-2}$ for the range of neutralino masses considered here;

(iii) To establish the range of m_χ to which Eq. (28) applies, one simply has to evaluate the lower bound m_χ by using Eq. (13);

(iv) The bounds, set by particle-physics measurements, on the two parameters $\tan\beta$ and m_A have a strong impact on the lower bound of m_χ [see Eq. (13)], but either have no effect (in the case of $\tan\beta$) or have a small effect (in the case of m_A) in the estimate of $\sigma_{\rm scalar}^{\rm (nucleon)}$.

Furthermore, we wish to notice that also the situation when relic neutralinos only provide a fraction of the CDM abundance is of great importance. Indeed, as shown in Ref. [54], in a direct detection experiment, relic neutralinos, whose relic abundance does not saturate the CDM abundance (that is, with $\Omega_\chi h^2 \leq (\Omega_{\rm CDM} h^2)_{\rm min}$), have a response larger than neutralinos of higher relic abundance. This property is due to the fact that, for subdominant neutralinos, the direct detection rate has to include a factor which appropriately depletes the value of the local DM density ρ_0 when $\Omega_\chi h^2 \leq (\Omega_{\rm CDM} h^2)_{\rm min}$. This *rescaling* factor $\xi = \rho_\chi/\rho_0$ is conveniently taken as $\xi = \min\{1, \Omega_\chi h^2/(\Omega_{\rm CDM} h^2)_{\rm min}\}$ [55]. Thus, effectively the relevant quantity to be inserted in the detection rate is not simply $\sigma_{\rm scalar}^{\rm (nucleon)}$ but rather $\xi\sigma_{\rm scalar}^{\rm (nucleon)}$. If one performs a scanning of the supersymmetric parameter space, it turns out that, at fixed m_χ, the quantity $\xi\sigma_{\rm scalar}^{\rm (nucleon)}$, when plotted including configurations with a subdominant relic density, can provide larger values than $\sigma_{\rm scalar}^{\rm (nucleon)}$ when the latter is plotted in the case when only neutralinos providing the observed DM density are included. This feature is manifest in the numerical results presented hereafter. These important rescaling properties are often overlooked in current phenomenological analyses of experimental data.

VI. CONSTRAINTS ON SUPERSYMMETRIC PARAMETERS FROM THE FERMILAB TEVATRON COLLIDER AND THE *B* FACTORIES

Now we discuss some relevant particle-physics measurements for which there have been sizable improvements recently, or which might become important in the near future as new data become available. We consider how each of the present experimental results on searches for new physics at the Tevatron and at the B factories can impact on the LNM $\mathcal{A}$ by putting constraints mainly on the two crucial parameters m_A and $\tan\beta$. Once these bounds are established, we determine how these limits reflect on the lower bound for the neutralino mass and consequently on the neutralino-nucleon cross section. Our analysis is performed analytically and numerically individually for each measurement, since the results of the various particle-physics experiments do not share the same level of reliability; actually, some of them are still presented by the experimental collaborations under the form of preliminary reports. Thus, in some case it is still premature to enforce the corresponding constraints at the present stage, though these might possibly become relevant in the future.

A. Search for the rare decay $B_s \to \mu^+ + \mu^-$ at the Tevatron

The SUSY contributions to the branching ratio for the decay $B_s \to \mu^+ + \mu^-$ are very sensitive to $\tan\beta$, since for high values of this parameter they behave as $\tan^6\beta$ [56–59]. Thus, the experimental upper bound on the branching ratio for $B_s \to \mu^+ + \mu^-$ can potentially put strict constraints on the elastic neutralino-nucleon cross section when this proceeds through a Higgs exchange, as is the case for the cross section in Eq. (26). However, we wish to stress here that the actual impact of these constraints depends dramatically on the specific SUSY model.

To clarify this point, we start discussing the features of the supersymmetric contributions to the branching ratio for $B_s \to \mu^+ + \mu^-$ which actually go like $\tan^6\beta$, as derivable for instance from Eqs. (1) and (2) of Ref. [57] (notice however that in the numerical evaluations of $BR(B_s \to \mu^+\mu^-)$ reported later on, all supersymmetric contributions are included as given in Ref. [56]). The dominant contribution which behaves as $\tan^6\beta$ reads

$$BR^{(6)}(B_s \to \mu^+\mu^-) \simeq \frac{1}{2^{12}\pi^3}\frac{G_F^2\alpha^2}{\sin^4\theta_W}\tau_B M_B^5 f_{B_s}^2 \left(\frac{m_\mu m_t m_{\chi^\pm}}{m_W^2 m_A^2}\right)^2 \times \left[1 + \left(\frac{m_b - m_s}{m_b + m_s}\right)^2\right]\sin^2(2\theta_{\tilde t}) \times |V_{tb}|^2|V_{ts}|^2\tan^6\beta \times [D(m_{\tilde t_2}^2/\mu^2) - D(m_{\tilde t_1}^2/\mu^2)]^2, \quad (29)$$

where τ_B is the B meson mean life, M_B is its mass, f_{B_s} is the B_s decay constant, m_t, m_b, m_s are the masses of the top, bottom and strange quarks, respectively; V_{tb} and V_{ts} are elements of the Cabibbo-Kobayashi-Maskawa matrix and the function $D(x)$ is defined as $D(x) = x\log(x)/(1-x)$. The structure of $BR^{(6)}(B_s \to \mu^+\mu^-)$ in Eq. (29) is due to the fact that the relevant amplitudes contain a one-loop insertion on a quark line, the loop being formed by a chargino (of mass $m_{\chi^\pm} \sim |\mu|$ in our models) and a stop whose mass eigenvalues are denoted as $m_{\tilde t_i}^2$ $(i = 1, 2)$; $\theta_{\tilde t}$ is the rotation angle which comes out when the stop squared-mass matrix is diagonalized. If in Eq. (29) we insert the values $\tau_B = (1.47 \pm 0.02) \times 10^{-12}$ sec, $M_B = 5.37$ GeV, $f_{B_s} = (210 \pm 30)$ MeV, $|V_{tb}| = 0.88 \pm 0.07$, and $|V_{ts}| = (38.7 \pm 2.1) \times 10^{-3}$, we obtain (by using the central values for the various quantities)

$$BR^{(6)}(B_s \to \mu^+ + \mu^-) \simeq 2.70 \times 10^{-6} \sin^2(2\theta_{\tilde{t}}) \left(\frac{m_{\chi^\pm}}{110\,\mathrm{GeV}}\right)^2 \times \left(\frac{90\,\mathrm{GeV}}{m_A}\right)^4 \left(\frac{\tan\beta}{35}\right)^6 \times [D(m^2_{\tilde{t}_2}/\mu^2) - D(m^2_{\tilde{t}_1}/\mu^2)]^2. \quad (30)$$

The uncertainty in the numerical factor in front of the right-hand side of this equation is of about 40%.

Since the purpose of the present discussion is essentially illustrative to show in which features the size of $BR^{(6)}$ in our LNM $\mathcal{A}$ may differ from its size in SUGRA models, we proceed to some approximations. In the scenario $\mathcal{A}$ of our model (see Sec. II) $|\mu|$ is typically small (close to the current LEP lower bound $|\mu| \gtrsim 100$ GeV) at variance with what occurs in SUGRA models, where the SUSY breaking implies larger values of $|\mu|$; then here the ratios $m^2_{\tilde{t}_{1,2}}/\mu^2$ are large: $m^2_{\tilde{t}_{1,2}}/\mu^2 \gg 1$.

Since $D(x) \simeq -\log(x)$ when $x \gg 1$, one obtains

$$[D(m^2_{\tilde{t}_2}/\mu^2) - D(m^2_{\tilde{t}_1}/\mu^2)]^2 \simeq [\log(m^2_{\tilde{t}_2}/m^2_{\tilde{t}_1})]^2. \quad (31)$$

Neglecting the contributions of the D terms, the stop-mass eigenvalues are approximately given by

$$m^2_{\tilde{t}_{2,1}} = m^2_{\tilde{q}} + m^2_t \pm m_t(A m_{\tilde{q}} + \mu/\tan\beta). \quad (32)$$

In scenario $\mathcal{A}$, where $\tan\beta$ is large and $|\mu|$ is small, unless the trilinear coupling is practically null, we have $|A| \gg |\mu|/(m_{\tilde{q}} \tan\beta)$ and consequently,

$$m^2_{\tilde{t}_2}/m^2_{\tilde{t}_1} \simeq 1 + \frac{2|A| m_t m_{\tilde{q}}}{m^2_{\tilde{q}} + m^2_t}. \quad (33)$$

By inserting Eq. (31) and (33) into Eq. (30) and taking into account that in our model $\sin^2(2\theta_{\tilde{t}}) \simeq 1$, we obtain

$$BR^{(6)}(B_s \to \mu^+ \mu^-) \simeq 5.8 \times 10^{-8} \left(\frac{14 A m_t m_{\tilde{q}}}{m^2_{\tilde{q}} + m^2_t}\right)^2 \times \left(\frac{m_{\chi^\pm}}{110\ \mathrm{GeV}}\right)^2 \left(\frac{90\ \mathrm{GeV}}{m_A}\right)^4 \left(\frac{\tan\beta}{35}\right)^6, \quad (34)$$

where the numerical coefficient in front of the right-hand-side is normalized to the experimental upper bound at 95% C.L., $BR(B_s \to \mu^+ \mu^-) \leq 5.8 \times 10^{-8}$ [40] (this is the latest published value by the CDF Collaboration; a somewhat smaller value is reported in unpublished CDF Public Note 9892 [60]).

Thus, neutralino configurations with a trilinear coupling parameter

$$|A| \lesssim \frac{1}{14} \frac{m^2_{\tilde{q}} + m^2_t}{m_t m_{\tilde{q}}} \lesssim 0.36 \quad (35)$$

are compatible with the constraint imposed by the upper bound on the branching ratio of the $B_s \to \mu^+ + \mu^-$ process. In the last step we have taken $m_{\tilde{q}} \simeq 1$ TeV. We recall that, because of the uncertainties involved in the determination of the numerical factor in Eq. (30), the numerical coefficients in Eq. (35) are affected by an uncertainty of about 20%. In addition, the approximation of Eq. (31) is only partly valid, since in our scenario the arguments $x_i = m^2_{\tilde{t}_{1,2}}/\mu^2$ of the $D(x)$ function are large but not exceedingly large and a further correction is at hand: a careful analysis shows that the value in Eq. (34) is actually reduced by a factor $\eta = (0.75 \div 1)$, for $x_i = (10 \div 100)$. This implies that the range on $|A|$ given in Eq. (35) can extend to values larger by a factor $\eta^{-1/2}$, i.e., $|A| \lesssim (0.36 \div 0.42)$.

We will see now that the situation is even more favorable than the one depicted in Eq. (34), once the role of the other SUSY contributions concurring to the full calculation of $BR(B_s \to \mu^+ \mu^-)$ is taken into account. In Figs. 3 and 4 we show the absolute value of the Wilson coefficients for each SUSY contribution to the $BR(B_s \to \mu^+ \mu^-)$ (colored points), compared to the full calculation of the dominant term (black points) (for expressions of these quantities see Refs. [56–59]), for our full scan in LNM $\mathcal{A}$. The sign of each term is indicated in parenthesis as "[+]" and "[−]." We see that also some other terms (notably, the W boson, the Higgs and the penguin diagrams) can contribute significantly, some with opposite signs, to the total branching ratio. The result of the full calculation when compared with the approximate expression of Eq. (34) is shown in Figs. 5 and 6. For models with light neutralinos,

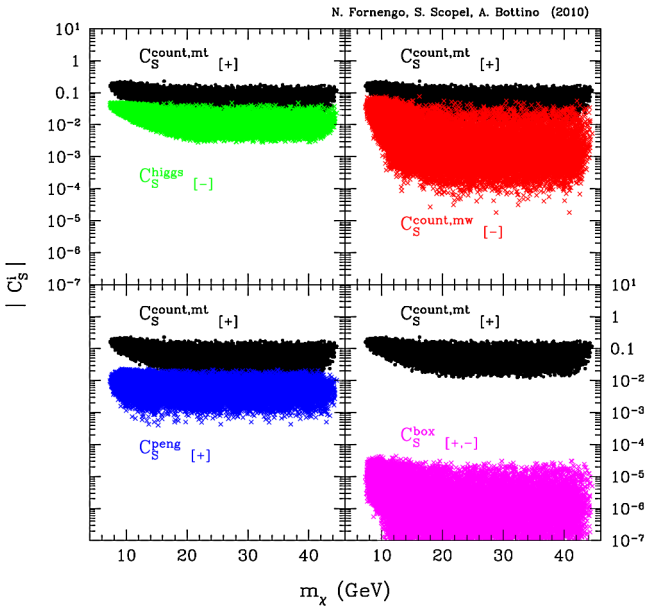

FIG. 3 (color online). Scatter plot of the absolute value of the Wilson coefficients $|C^i_S|$ for each SUSY contribution to the $BR(B_s \to \mu^+ \mu^-)$ (colored points), compared to the full calculation of the dominant term (black points) (for expressions of these quantities see Refs. [56–59]), for the LNM-$\mathcal{A}$ scan. The sign of each term is indicated in parenthesis as "[+]" and "[−]". The values of $|C^i_S|$ are plotted as functions of the neutralino mass m_χ.

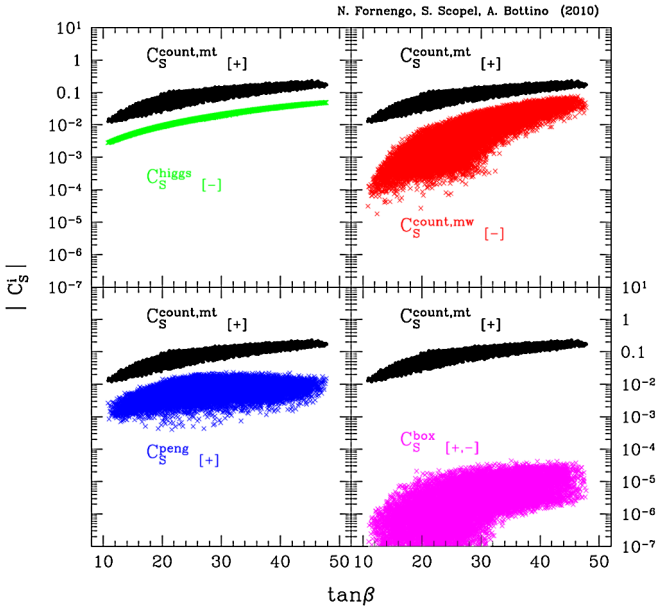

FIG. 4 (color online). The same as in Fig. 3, except that the Wilson coefficients $|C_S^i|$ are plotted as functions of tanβ.

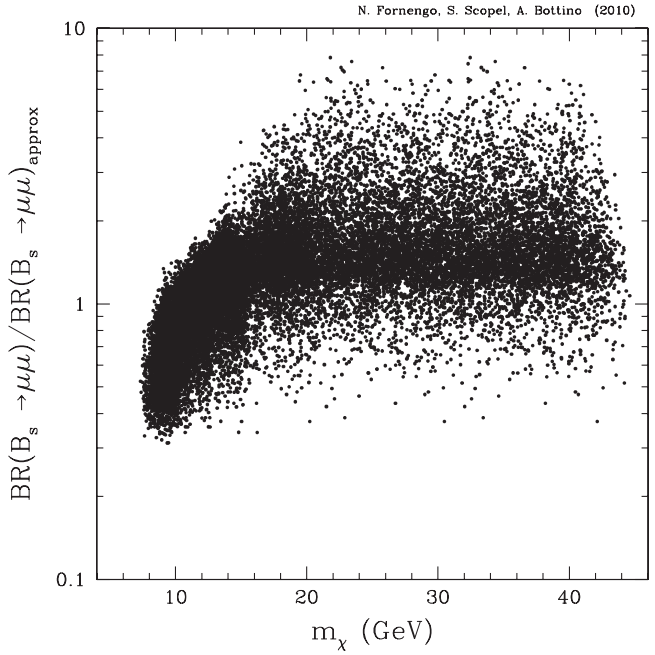

FIG. 5. Scatter plot of the ratio between the full numerical calculation of $BR(B_s \to \mu^+\mu^-)$ and the approximate expression of the dominant term $BR^{(6)}(B_s \to \mu^+\mu^-)$ given in Eq. (34), for the LNM-$\mathcal{A}$ scan. The scatter plot is shown as a function of the neutralino mass m_χ.

especially in the case of $m_\chi \lesssim 10$ GeV, the full calculation can be smaller that the approximate one by up to a factor of 3.

Figure 7 shows the correlation between tanβ and the trilinear parameter A in the LNM-$\mathcal{A}$ scan. We remind that

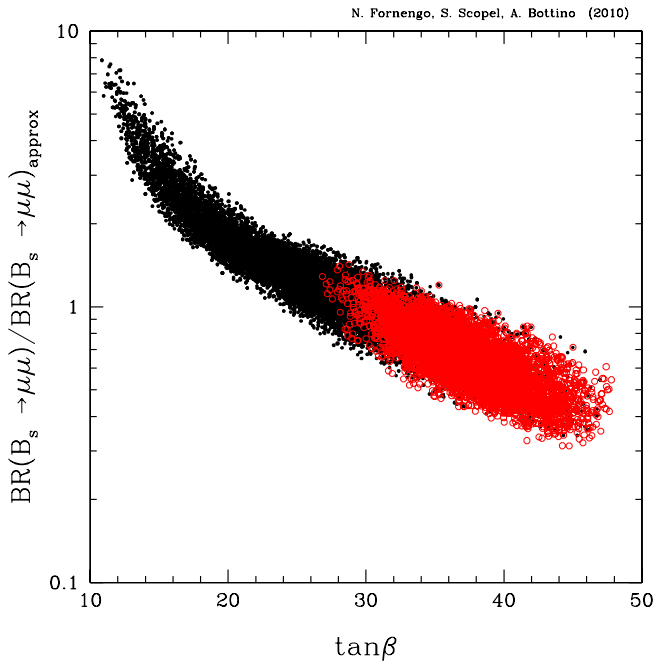

FIG. 6 (color online). The same as in Fig. 5, except that the scatter plot is shown as a function of tanβ.

here, as in all figures, the bound $BR(B_s \to \mu^+\mu^-) < 5.8 \times 10^{-8}$ is implemented. We see that, because of the competition among various contributions, the range of A for light neutralinos (red circles) is wider than the one derived in Eq. (35) and can extend up to about 0.6.

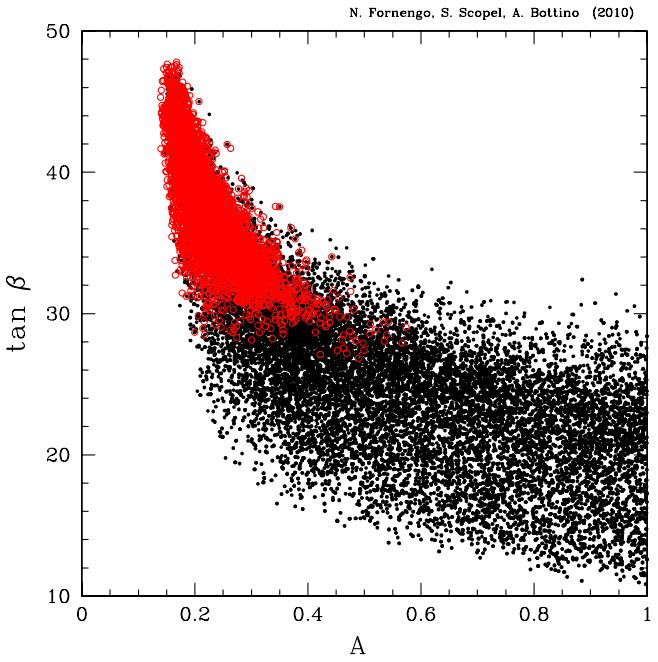

FIG. 7 (color online). Scatter plot which shows the correlation between tanβ and the trilinear parameter A, for the LNM-$\mathcal{A}$ scan. Black points refer to $m_\chi > 10$ GeV, red circles to light neutralinos with $m_\chi \leq 10$ GeV.

Taking into account the requirements on $|A|$ used in deriving the previous analytical approximations, i.e.,$|A| \gg |\mu|/(m_{\tilde{q}} \tan\beta)$, and the upper bound of Eq. (35), we find that $|A|$ has to satisfy the conditions

$$\frac{|\mu|}{m_{\tilde{q}} \tan\beta} \ll |A| \ll \frac{m_{\tilde{q}}}{m_t}, \tag{36}$$

i.e., a hierarchy which is naturally realized (i.e., no fine-tuning is involved) in our model where the values of the parameters are defined at the EW scale and not induced by SUGRA conditions.

A demonstration of how this hierarchy is actually realized is provided by the numerical results in Fig. 8. The three separate regions correspond to the numerical values for the three quantities specified in the picture and in Eq. (36). The (colored) circles denote the neutralino configurations with $m_\chi \leq 10$ GeV.

As discussed in the literature [41,42], a supersymmetric contribution leading to an increase of the decay rate of the process $B_s \to \mu^+ + \mu^-$ is correlated to a decrease of the difference $\Delta M_{B,s} \equiv M_{B_s} - M_{\bar{B}_s}$, compared to the value expected in the standard model, $\Delta M_{B,s}^{\rm SM}$. In Fig. 9 we show a scatter plot of the ratio $R_{\Delta M_{B,s}} = \Delta M_{B,s}^{\rm SUSY}/\Delta M_{B,s}^{\rm SM}$ as a function of m_χ for the LNM-$\mathcal{A}$ scan. Taking into account that $R_{\Delta M_{B,s}} = 0.80 \pm 0.12$ [42], which at 95% C.L. implies an allowed range $0.57 < R_{\Delta M_{B,s}} < 1.03$, one sees that the quantity $\Delta M_{B,s}$ does not imply any additional constraint on the LNM parameter space.

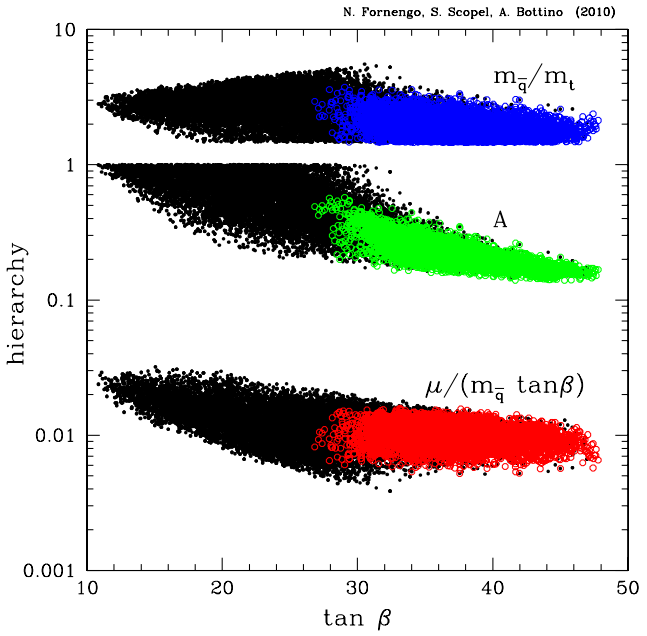

FIG. 8 (color online). Scatter plot which shows the hierarchy of Eq. (36) in the LNM-$\mathcal{A}$ scan. The three separate regions correspond, from top to bottom, to the numerical values for the three quantities $m_{\tilde{q}}/m_t$, A and $\mu/(m_{\tilde{q}} \tan\beta)$. Colored circles denote the neutralino configurations with $m_\chi \leq 10$ GeV.

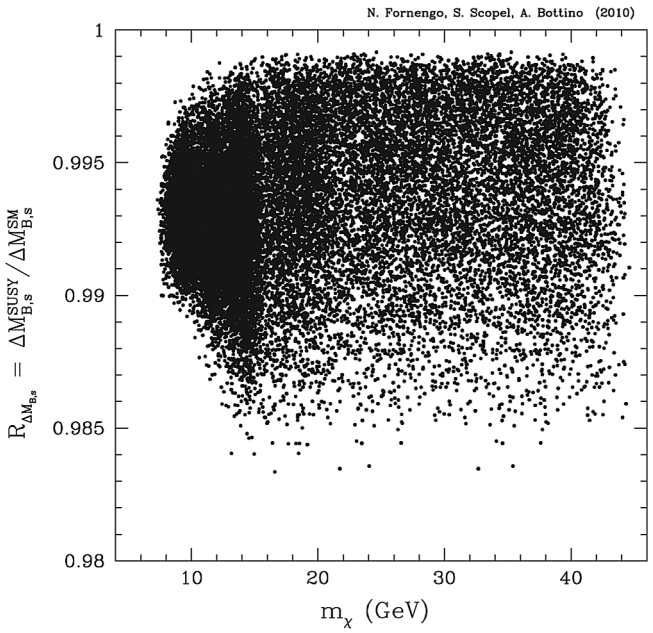

FIG. 9. Scatter plot of the ratio $R_{\Delta M_{B,s}} = \Delta M_{B,s}^{\rm SUSY}/\Delta M_{B,s}^{\rm SM}$ as a function of m_χ, in the LNM-$\mathcal{A}$ scan.

To summarize the results of the previous discussion, we can say that in the LNM the upper bound on the branching ratio of the $B_s \to \mu^+ + \mu^-$ process is not significantly constraining, due to the relatively small values of the chargino mass and a small splitting between the two stop masses. These are situations which are naturally obtained in our LNM, contrary to the situation that occurs in SUGRA-like models, as the one considered in Ref. [15]. It is then erroneous to interpret the results of Ref. [15] as valid also for a generic effective MSSM with light neutralinos, as is sometimes done in recent literature (see for instance Refs. [21,23]).

B. Search for neutral MSSM Higgs bosons at the Tevatron

The Tevatron is expected to have a good sensitivity to the search for Higgs neutral bosons in the regime of small m_A and large $\tan\beta$, since in this region of the supersymmetric parameters the couplings of the neutral Higgs bosons $\phi = h, A, H$ to the down fermions are enhanced. This has prompted searches by the CDF and D0 Collaborations for the neutral Higgs bosons which decay as $\phi \to b\bar{b}$ or $\phi \to \tau\bar{\tau}$ (for an updated review see Ref. [61]).

We report here the results of these collaborations in terms of upper bounds on $\tan\beta$ versus m_A. These bounds are displayed in Figs. 10–12 as piecewise linear paths.

The D0 Collaboration has determined upper bounds for the production rate of the process $p\bar{p} \to \phi \to \tau^+\tau^-$ (inclusive $\tau^+\tau^-$ production) in Ref. [37] and for the $\tau^+\tau^-$ production in association with a b quark in Ref. [38] and then converted these bounds into upper limits for the SUSY parameters $\tan\beta$ and m_A. These limits are represented in